

# AEROACOUSTIC NOISE MEASUREMENTS IN AERODYNAMIC LOW-SPEED WIND TUNNELS

**Takeshi ITO\***, **Hiroki URA\***, **Yuzuru YOKOKAWA\***  
\* Japan Aerospace Exploration Agency

**Keywords:** *Aerodynamic noise, Phased-array, Low-speed wind tunnel, High-lift device*

## Abstract

*Using phased-array microphone technique, we obtained aerodynamic data in closed test section of conventional aerodynamic wind tunnels. Especially, large-scale testing was able to be carried out, and detailed testing was successfully completed. These aerodynamic data was able to be discussed with considering the corresponding aerodynamic data directly including quantitative acoustic contribution of airframe elements. This testing technique should be very important feature as the present and future aerodynamic and aerodynamic design.*

## 1 Introduction

To evaluate aerodynamic noises from airframe of civil aircraft using ground testing facilities, measurement techniques for anechoic low-noise wind tunnels have been developed and generally used. However, this type of aerodynamic measurements is carried out in the different condition as aerodynamic force measurement. These wind tunnels usually have open-jet type test sections, and can measure the noise of tested models from outside of the flow at the test section. The open-jet flow is normally very different from aerodynamic testing condition, especially, in high-lift configuration which deflects the uniform flow. Moreover, deflected open-jet might cause strong noises at the collector of the jet in downstream position, and sometimes this background noise hides the target noise in the test section.

To solve these problems, some aerodynamic testing in closed test section have been conducted.[1,2] We also started an aerodynamic-noise measurement project in aerodynamic low-

speed wind tunnels from 2004 in Japan Aerospace Exploration Agency (JAXA). Our concepts of the measurement are (1) noise measurement in a closed test section, (2) simultaneous measurement of aerodynamic and aerodynamics, (3) noise source visualization. To realize these concepts, phased-array microphones which were flush-mounted on the wall surface of the test section were applied. In these days, noise source visualization technique has been commonly used, but application for closed test section in the aerodynamic noisy wind tunnel is still a challenging target and there are many technical problems such as mounting and arrangement of microphones, background noise of fan, support of model, aerodynamics-like data-processing for simultaneous measurement, and so on.

In this paper, aerodynamic measurement system with phased-array microphones in closed test sections of 6.5m x 5.5m Low-speed Wind Tunnel (LWT1: Fig. 1a) and the 2m x 2m Low-speed Wind Tunnel (LWT2: Fig. 1b) in JAXA in order to obtain aerodynamic data and aerodynamic data simultaneously are introduced. Measurement results such as trailing-edge noises, high-lift device noises, and gear noises from airframe will be shown.

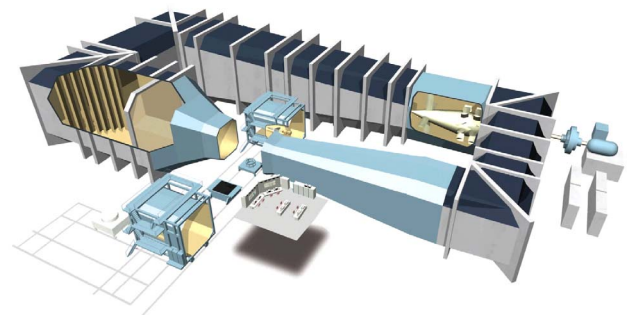


Fig.1a. 6.5m x 5.5m Low-speed Wind Tunnel in JAXA (LWT1)

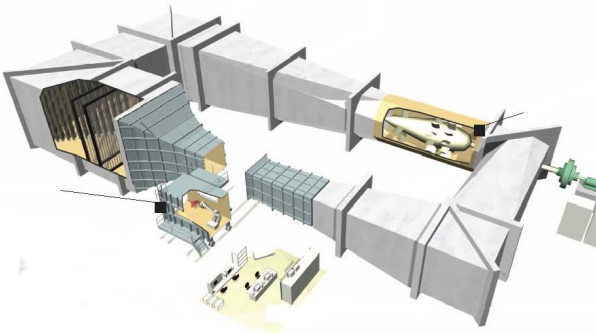


Fig.1b. 2m x 2m Low-speed Wind Tunnels in JAXA (LWT2)

## 2 Phased-array microphones in Low-speed Wind Tunnels

### 2.1 Aerodynamic Wind Tunnels in JAXA

In JAXA, we have two types of low-speed wind tunnels. Those are 6.5 m x 5.5 m Low-speed Wind Tunnel (LWT1), and 2 m x 2 m Low-speed wind tunnel (LWT2).

The JAXA-LWT1 (Fig. 1a) has been used to obtain low-speed aerodynamic performance and flow field around aircraft during take-off and landing, and low speed flight condition. The maximum wind speed is 70 m/s at the test section. This tunnel is operated in atmospheric pressure condition. The test section is the largest in Japan as low speed wind tunnel for aircraft. The length of the closed circuit is 200 m at total, and the long leg and short leg is 75 m and 25 m, respectively. Since the completion in 1965, many wind tunnel tests, such as vertical and short takeoff and landing (V/STOL) aircraft, low-speed aerodynamic research and development, conventional aircraft, and space vehicles, have been conducted. This wind tunnel has two types of support system for experimental model, which are a strut support with pyramid-type force balance and a sting support with internal force balance. Sometimes half-span models with external force balance are used without support system. Aerodynamic force and pressure have been measured to obtain performance and characteristics of those models, but also some flow visualization techniques such as oil flow, china clay, and tuft are also able to be used.

The other smaller-size low-speed wind tunnel, JAXA-LWT2 (Fig. 1b), is also a closed circuit type and conventional wind tunnel built in 1971. Its circuit length is 96 m, and its test section has cross-section of 2m x 2m and length of 4 m. In addition, this wind tunnel has characteristics of maximum wind speed of 67 m/s and relatively low turbulent level of 0.06 %. A testing model is supported by strut from a lower wall. 6-component force can be measured with pyramid type balance changing the angle of attack and side slip angle. Models can be also supported by sting with robot, and aerodynamic forces are able to be measured using internal force balance. Half-span model on the lower wall are sometimes used on the external-type 4-component force balance. This tunnel has been used for a variety of tests from basic aerodynamic research to tests for flutter tests, boundary-layer control, powered-lift STOL aircraft tests, and so on because of its characteristics of little turbulence and relatively low noise and also appropriate size of test section and this tunnel has also a gust-wind test cart in which added load and flight movement in a gust-wind force can be measured. Recently, high-lift device (HLD) research is one of the most important purposes in those wind tunnels to develop high-performance HLD for civil aircraft development.

### 2.2 Wall-Mounted Microphone Array in Closed Test Section

It is very important to measure aerodynamic noise in those aerodynamic wind tunnels, because we can obtain the same flow field for aeroacoustic measurement as the aerodynamic testing. For this purpose, we put arrayed microphones of 1/4-inch on the side wall or ceiling of the closed test section for LWT1 and LWT2. Noise source survey was realized with delay-and-sum beamforming method for measured data of phased-array microphones to avoid background noise of aerodynamic wind tunnel and reflection in the closed test section.[3-4]

As shown in Fig.2 and Table 1, our phased-array microphone system consisted of 48 microphones (32 for NACA0012) of B&K type

4951, 3 units of conditioning amplifier (B&K type 2694A), A/D converter (NI PXI-4462) and PC (NI 8351). The microphones have diameter of 7 mm, their frequency range of 10 Hz to 20 kHz and their dynamic range of 30 dB to 140 dB. Conditioning amplifier has frequency range of 0.1 Hz to 50 kHz and amplifier gain of -10 dB to +40 dB. This A/D converter has 24 bit resolution and maximum sampling rate of 204.8 kSamples/s. Each microphone was calibrated by piston phone (B&K type 4228) before airframe noise measurements were conducted. In this research, measurement data of noise were processed by using sensitivities of microphones which were obtained by the calibration.

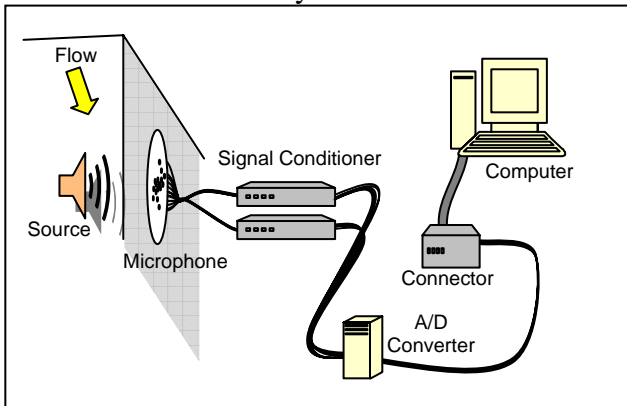


Fig. 2. Phased-array measurement system

Table 1 Specification of measurement system

Item	Number	Spec.
Microphone	48 or 32	1/4-inch, 10Hz~20kHz, 30~140dB B&K Type 4951
Amp./Signal conditioner	3	16ch, HPF1Hz, LPF50kHz, Gain: -10dB~+30dB
A/D	12	4ch, 24bit, 200kHz sample hold

We applied multi-arm-spiral method for arrangement of microphones and optimized characteristics of array to be able to measure noise data at a wide range of frequency. The samples of arrays with multi-arm spiral arrangement as shown in Fig. 3, which were placed on side-wall or ceiling of the test sections are shown in Figs.4, 7, 13, 15, 21, 25.

The microphone array was covered by Polyurethane-foam sheet to avoid aeroacoustic noise on the microphone screen generated by interaction of uniform flow in wind tunnel. These systems were able to measure at the one-

third octave band frequency about 800Hz to 16 kHz. We used data processing technique of conventional beamforming which was modified to reduce effects of background noise without test model. Airframe noise was able to be measured by using this data-processing method under the condition of large level of background noise in which airframe noise was not able to be measured by using normal conventional beamforming. Survey area of noise source was 1500 mm-square for LWT2 to 5000mm-square for LWT1. The gain by the simulation was about -6 ~ -10 dB from source to side robes, which was sufficient to distinguish the source from side robes.

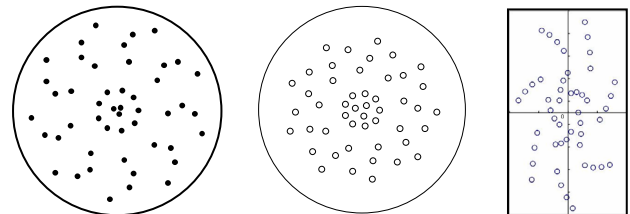


Fig. 3. Samples of multi-arm phased-array microphone arrangements.

### 3 Testing results in LWT2

#### 3.1 Trailing Edge noise on NACA0012

At first, our microphone array system has been developed in LWT2 because of the adequate size of handling and simplicity of the experimental model. To confirm the aeroacoustic noise measurement system using simple aeroacoustic noise generation phenomena, two-dimensional NACA0012 wing section model was tested in LWT2.[5]

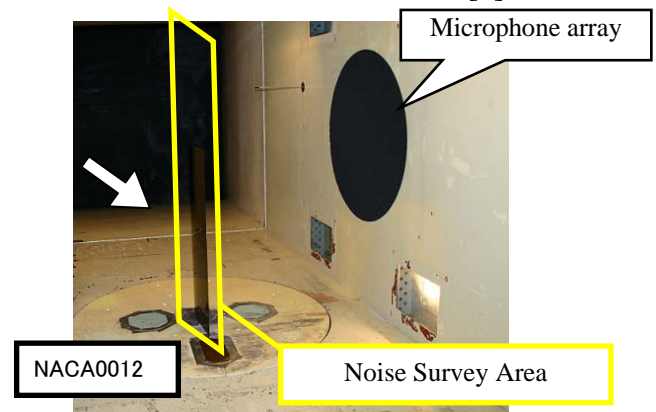


Fig.4. NACA0012 wing section in LWT2.

The span of model was 1000mm, and the chord length was 400mm. the model was placed on the lower surface of the wind tunnel wall vertically as shown in Fig. 4. This NACA0012 wing model caused the well-known trailing edge noise (TE noise), and it was suitable to confirm and perform the measurement system.[6-7] 32 microphones were used for this testing as a first step in our wind tunnel testing.

In Fig. 5a, SPL results and noise source visualization from as change of angle of attack at 50 m/s are shown. Some of peaks were observed, but those peaks were difficult to find out whether it came from testing model or from other part of wind tunnel. However, using noise source visualization technique as shown in Fig. 5b-f, it was found that 1303 Hz was aerodynamic noise from the model. On the other hand, other peaks on SPL plot were not aerodynamic noise but background noise from the wind tunnel. The noise source moved from spanwise direction as increasing of angle of attack. This meant that the three-dimensional flow was caused because the model had a wing tip, although the TE noise should occur two-dimensionally by some aerodynamic phenomena such as small separation at the trailing edge, boundary layer transition on the surface and the Karman vortex by the shear layer from the trailing edge.

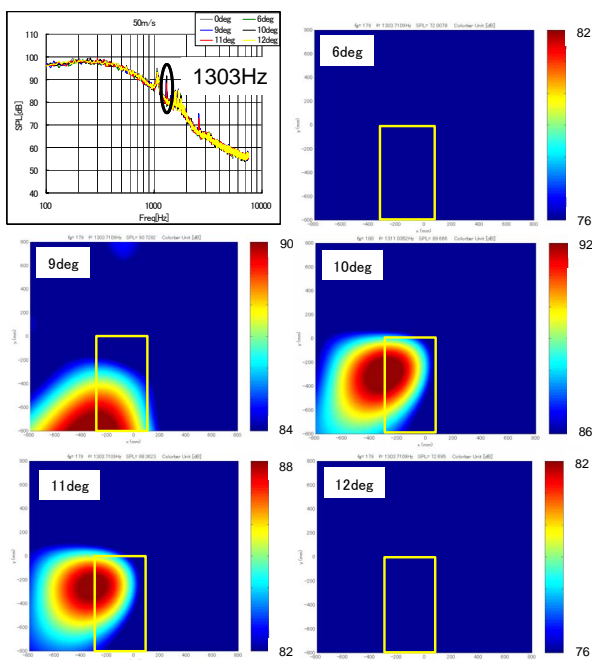


Fig.5. Trailing edge noise from NACA0012.

Some flow field investigations such as oil flow visualization and boundary layer measurement using hot film were applied to confirm that the noise source was TE noise and to make the phenomenon clear. These aerodynamic measurements worked well in our aerodynamic wind tunnel. Detailed experimental results are shown in reference [5]. The results were analyzed and mechanism of noise generation was discussed, and it was found that the noise source visualization results were reasonable.

### 3.2 High-Lift-Device Model (OTOMO)

In JAXA, research for airframe noise from high-lift device (HLD) has been started to obtain their design approach to achieve both low noise and aerodynamic high performance. To reduce airframe noise from high performance HLD, basic characteristics of aerodynamics and aeroacoustics have to be understood in detail. For this research, aeroacoustic noise and aerodynamic characteristics have to be measured simultaneously. Therefore, our microphone array system, external force balance, and electric scanning pressure (ESP) measurement system of LWT2 are very useful, and were applied for the research to evaluate aerodynamics and aeroacoustics of HLD. A simplified three-element wing model was able to be investigated in LWT2 using these aeroacoustic and aerodynamic measurements in order to better understand relationship between airframe noise and the phenomena of flow field around HLD.[8-11]

Figure 6 shows the model for aeroacoustic research of high-lift device (OTOMO) in LWT2. This model was tested to clarify basic phenomena of noise generation at wing tip, flap tip, and slat including its cove, and to reduce those noises by applying modification of the configuration. The model had 0.6 m in chord length, 1.4 m in wingspan, no sweep-back angle, no taper, and no dihedral angle. There were full-span leading-edge slat, and 70 %-span single-slotted flap at trailing-edge. The model had 189 static pressure taps. This model was placed on external-type 4-component force balance, and aerodynamic force was measured. Basic characteristics are also shown in Fig. 7. The

performances of high lift device were demonstrated as increase of lift coefficient and stall angle of attack.

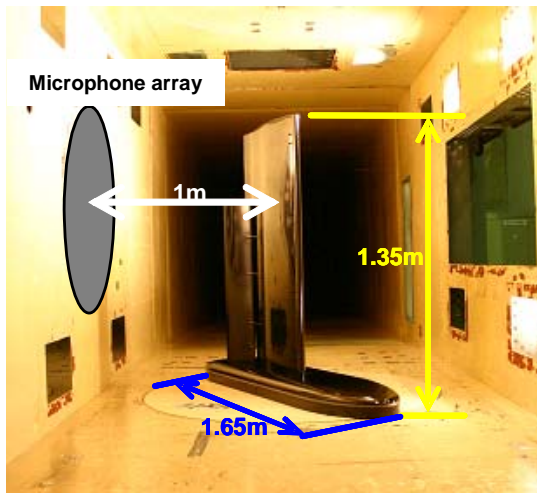


Fig.6. High-lift device model (OTOMO)

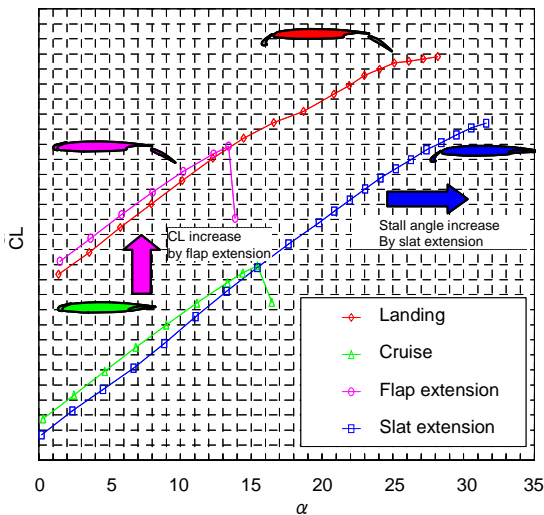


Fig.7. aerodynamic characteristics of OTOMO

Figure 8 shows the typical results of noise source visualization with beamforming at the landing configuration. In the relatively low frequency at 4 kHz, the some noise sources were clearly observed at main-wing tip, flap-tip and slat in lower angle of attack, as shown in Fig. 8(a). On the other hand, a dominant and larger noise source was visible in main-wing tip at higher angle of attack in Fig. 7(c). In the higher frequency at 12.5 kHz, there was span-wise noise source distribution at slat region as shown in Fig. 7(b) and 7(d). According to the results obtained each measurement, noise in middle frequency range seemed to be mainly governed by main-wing tip and flap-tip. At high

frequency range, slat seems to be dominant noise source, but the noise source pattern of span-wise distribution depended on angle of attack.

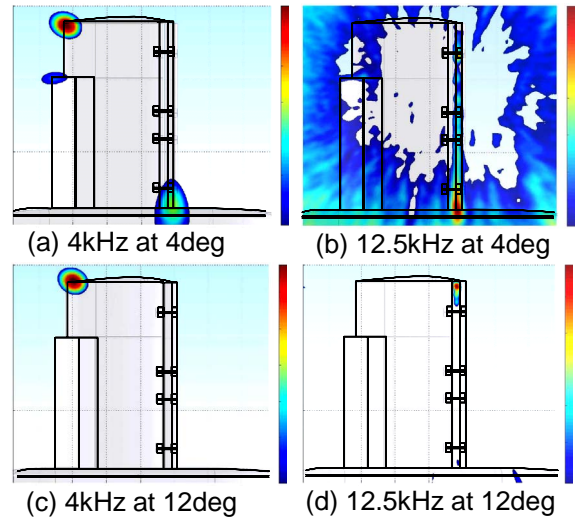


Fig.8. Noise source on High-lift devices.

To clarify the characteristics of noise from each wing element more in detail, local maximum value was surveyed within three regions as shown in Fig. 9, and then this was used as the typical noise source level of each wing element.

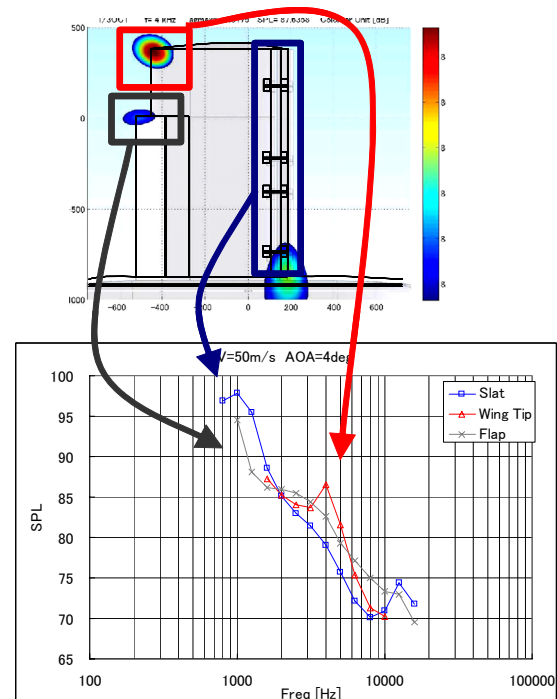


Fig.9. Noise element characteristics on OTOMO

Here, each noise spectrum was evaluated by using local maximum value as the first step of quantitative analysis, although area effects of noise distribution will be evaluated as a future

work for absolute noise source level analysis. From this evaluation, noise characteristics of each element of the wing, such as slat noise, wing-tip noise, and flap-side-edge noise were able to be separately analyzed and discussed as changing frequency and angle of attack. For example, the strong slat noise was observed above 10 kHz, wing tip made narrow band noise about 4 kHz, flap tip became remarkable at around 8 kHz, and so on.

To compare with normal aeroacoustic testing facility, the correction of aerodynamic wall interference had been tried by compared with test results of the same model at open-jet test section of Large-scale Anechoic Wind Tunnel in Railway Technical Research Institute (RTRI). The data of LWT2 and RTRI were correlated by surface pressure distributions of the model. Fig. 10 shows comparison of  $C_p$  distribution at 25 % spanwise cross section. The geometric angle of attack of RTRI was 8 deg at landing configuration, and those of LWT2 were about 4 deg. In order to investigate the ratio of airframe noise from each wing element to overall airframe noise, noise data of far-field in RTRI and noise source visualization in LWT2 were compared at the above condition. Then absolute sound pressure levels were evaluated by estimation of each noise source at RTRI from the ratio of sound power of each noise source to integration value at LWT2 as shown in Fig. 11. This estimation included some correction such as distance effect, reflection effect, and so on, and now we have obtained one of the useful methods of correction for LWT2 noise data.

Those aeroacoustic evaluations about high-lift devices including aerodynamic discussion are shown in reference [9-11], and they are very important and useful for to be modified to achieve the favorable reduction of the noise.

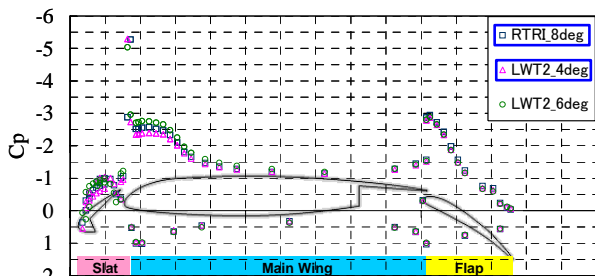


Fig.10. Pressure distribution on wind surface in LWT2 and RTRI characteristics

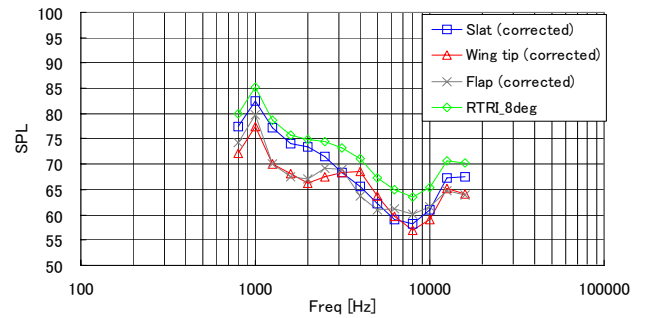


Fig.11. Noise SPL correction using overall noise level in RTRI

### 3.3 Landing gear noise using sting support

Landing gear is also very important from a view point of aeroacoustic noise of aircraft.[12,13] Preliminary study for research and development of noise from landing gear which should be seriously investigated in the near future was carried out by using lifting-body configuration model with several types of landing gear.[14] This model was supported by six-degree-of-freedom robot arm support system at roll angle of -90 deg as shown in Fig. 12. Although the robot support system is very convenient and useful for aerodynamic testing, the robot arm

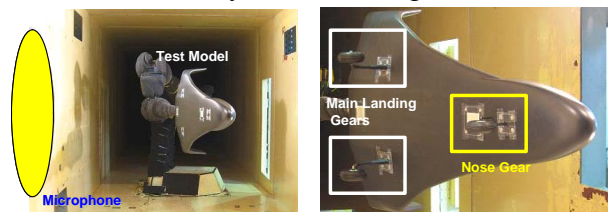


Fig.12. Landing gear testing with sting support in LWT2

should cause aeroacoustic noises due to its complicated mechanical configuration and affect the aeroacoustic measurement, especially, in the non-anechoic test section. Therefore, noise reduction treatment for the support system was very important technique for the measurement, and it was covered by acoustic absorbent to reduce noise from the support system.

Fig. 13 shows typical measurement results of baseline landing gear noise at angle of attack of 0 deg at 50 m/s and frequency of 6.3 kHz. SPL of the noise generated by main landing gear is about 4 dB larger than one generated by nose gear. The ratio of S/N seemed to be relatively lower than other cases due to background noise

by the sting support system. Focusing attention on a source location of noise from nose gear, maximum value of SPL exists on outboard side of nose gear, and there is junction between wheel and strut. Maximum value of SPL of the noise source from main landing gear was also located on junction between wheel and strut. This detailed identification of noise location was very remarkable and important feature of our microphone array technique. From results of this series of experiments, the effects of the number and size of wheel, main leg door, an inner space of wheel on sound pressure level and frequency of the noises were also better understood. We were able to obtain important knowledge of the characteristics of landing gear noises.

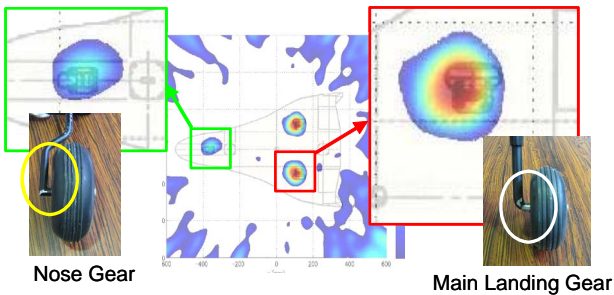


Fig.13. Detailed noise survey of landing gears

## 4 Testing results in LWT1

### 4.1 Half-span High-lift Configuration Aircraft Model (JSM)

As a research program to make design methodology for advanced high-lift system, a half-span model of a realistic aircraft configuration equipped with leading-edge slat, flaps, fuselage, nacelle-pylon, slat tracks and flap track fairings was tested.[15] Not only aerodynamic data, but also aeroacoustic noise sources were observed by using phased-array microphone. Here, we used flash mounted 48-microphones on the side wall of the test section, as shown in Fig. 14.[16] The array was placed on the side wall, but the testing model was located at lower part of test section. To obtain directivity for the noise survey toward lower direction, the longwise shape of array was designed. Also, the noises were transmitted in

the uniform flow, so it was reasonable that the array was shifted to downstream direction

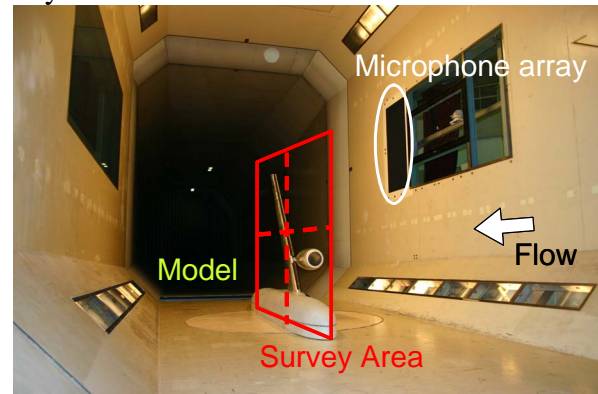


Fig.14. Large-scale half-span model for high-lift device testing

Figure 15 shows lift coefficient of this model by measured with external-type 5-component force balance. It was important that the aerodynamic force data obtained simultaneously with aeroacoustic data. Here, acoustic characteristics

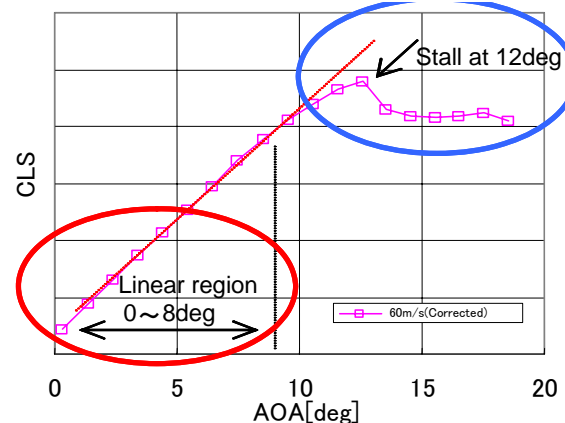


Fig.15. Aerodynamic characteristics of the model

of this experiment will be discussed about of linear region and stall region.

Figure 16 shows noise source survey results around the testing model. Noise sources from high-lift devices and nacelle-pylon were obtained clearly. At 4 deg of angle of attack in linear region in Fig. 16(a), strong noise from flap tip was observed. Vortices at the flap tip caused noise by interaction to the flap surface at this angle. But the relatively small noise was observed at the tip of main wing. One of the reasons was that the shape of the wing tip was rounded and the vortex was weaker than flap tip, so the noise became smaller. Some noises from slat tracks were also obtained, but no slat noise. Some calculations and experiments show that well-known slat noise occurs at much higher

frequency, so the frequency of this result might be too low to observe the slat noise here. At this angle of attack, noise from slat-pylon region was also observed, but it was not very strong.

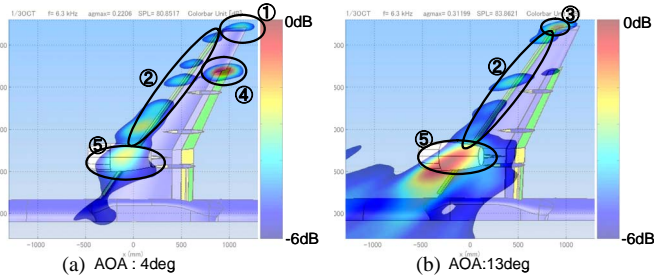


Fig.16. Noise visualization on the high-lift devices on the model

However, at 13 deg in stall region, the strongest noise was observed on the slat-pylon region as shown in Fig. 16(b). The image of the noise source was large because of not only the low resolution of the array but also relatively large size of noise source itself. The slat and nacelle-pylon region consisted of large pylon, slat edge and leading edge of main wing. Therefore, this slat-pylon region had a large-size opening of triangle shape among those components. This area should cause strong noise, and it was observed in this experiment.

This aeroacoustic phenomenon must also be related to the flow field around this region at this high angle of attack condition. It agreed with the oil flow results as an aerodynamic testing. Flow separation on the wing and flap happened. Therefore, the angle of attack must be too large to keep vortex to cause noises around the wing tip and flap tip. The flow separation was shown from pressure distribution as shown in Fig.17. There aerodynamic data were very important and useful to investigate mechanism of the noise occurrence as well as to understand flow structure.

Finally, Figure 18 shows element analysis of noise source. Flap noise was dominant at low angle of attack, slat noise increased at high angle of attack, and slat-pylon noise were large at all region, especially, high angle of attack. These results were reasonable considering aerodynamic measurements and discussions as abovementioned. Phenomena of flow field and mechanism of noise generation around high-lift devices at the landing configuration should be

very complicated to be analyzed. However, our aerodynamic and aeroacoustic measurement system was very powerful technique to investigate its characteristics. Detailed and quantitative characteristics were able to be discussed using data reduction of its noise level and comparing with aerodynamic force data which obtained simultaneously.

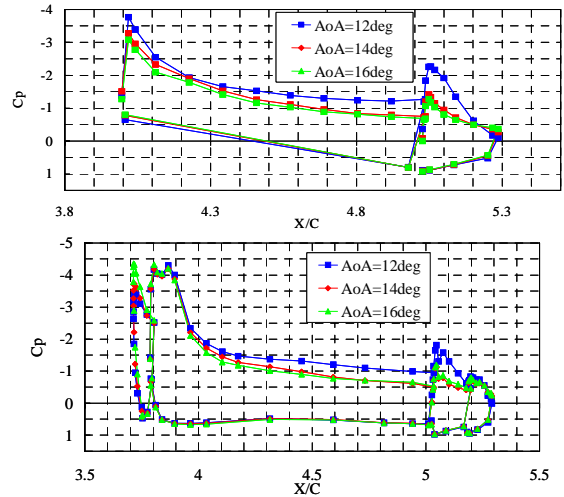


Fig.17. Noise visualization on the high lift devices on the model

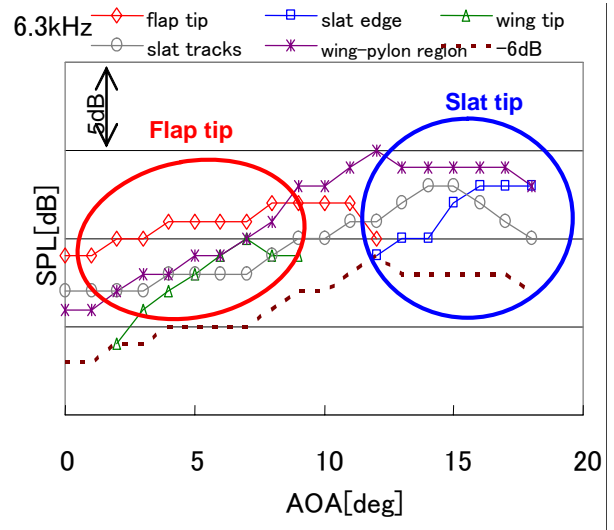


Fig.18. Noise element evaluations of HLD

## 4.2 Large-scale SST model with strut support.

This technique was applied to the development the SST airframe model, provided by the Boeing Company, was a full-span 6 % scale model of a double delta wing high-speed civil transport.[17] This was similar to the configuration of reference [18] but different



scale. A photograph of the model in the wind tunnel is shown in Fig. 19. Size of the model was approximately 5.8 m long, and had a wing span of approximately 2.4 m. The leading edge segment was deflected to 30 deg and the trailing edges of 10 deg were used as high-lift devices for landing configuration. The model had removable landing gear for gear configuration. Chine was attached on the both side of body near the nose as a vortex generator.

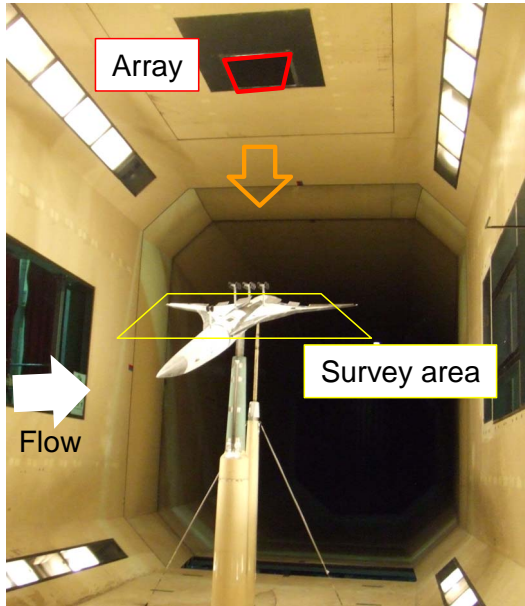


Fig.19. SST model with strut support

The model was supported as upside-down configuration from floor of the wind tunnel with main strut and aft strut, and microphones were mounted on the upper wall (ceiling) of the test section. The pivot point of the model was located on the tunnel centerline. The support allowed the angle of attack of the model. The strut was connected to the pyramid-type 6-component force balance. The aerodynamic force was able to be measured by the aeroacoustic measurement including little disturbance. Results of 40 m/s are shown here. Typical noise sources were obtained at landing-gear configuration in Fig. 20.

Strong noise from main gear was observed, although front gear did not cause any remarkable noises. The level of the noise by main gear was stronger than other noises at low angle of attack. Wing tips noise was generated by pressure difference between lower surface and upper surface with smooth flow on the wing.

This noise was observed only from 4 to 12 deg. It was caused at high-lift condition before stall phenomena. Chine noise was remarkable at very high angle of attack because of strong vortex at that angle. Noise from kink was strong at all frequency, although other noise disappeared at 16 kHz. The kink noise was caused by vortex interaction between leading-edge vortex on inner-wing and outer-wing., which might have shown the broad band noise due to complicated interaction between two vortexes. As shown above, it was found that the flow structures around the airframe elements such as gear, wing tip, chine, and kink, were very different, considering various characteristics of those noise sources.

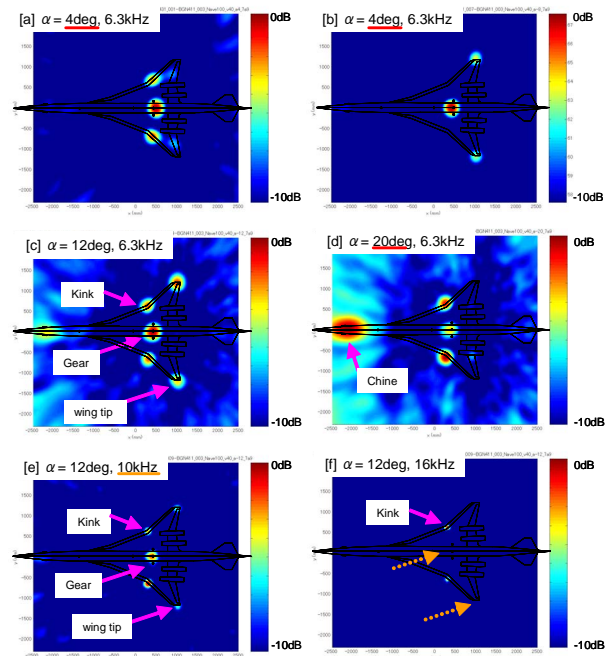


Fig.20. Typical noise sources on SST model at landing-gear configuration

Relative level of overall noise was useful to compare the many testing results as mentioned above. Here, each noise level of elements of noise sources was investigated from noise source survey for sweep of angle of attack in the landing-gear configuration, as shown in Fig. 21. At 6.3 kHz, the kink noise showed relatively high in noise level at small angle of attack, and also very high at large angle of attack. Especially, it was interesting that the peak of overall noise level at 18 deg of angle of attack was caused by the kink noise. The kink noise in large angle of attack region started to increase at

about 10 deg of angle of attack, and it was caused by flow separation on the main wing. Wing tip noise was also remarkable in medium angle of attack from 4 deg to 8 deg. Chine noise became large at the highest angle of attack, but it was still smaller than kink noise. These phenomena are same at 4 kHz and 10 kHz.

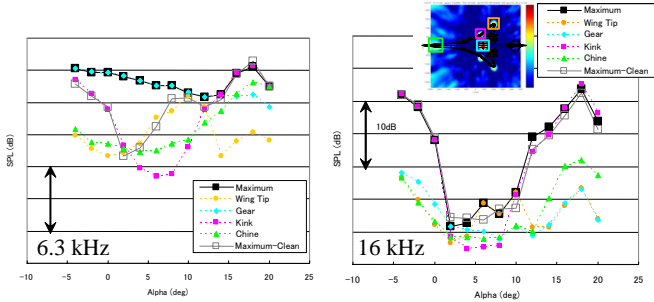


Fig.21. Noise element evaluation on SST model

At 16 kHz, the characteristics were very different. Gear noise was low in all angles of attack, and kink noise was remarkable in very low angle and high angle of attack. Thus, only kink noise dominated overall noise at 16 kHz. In different words, it is important that the characteristics of kink noise at 16 kHz were remarkable as same as other frequency which meant broad band noise, although gear noise was not visible at this frequency.

### 4.3 MRJ Aeroacoustic noise evaluation

In Japan, a 5-year R&D project has been in progress toward the development of an environment friendly high performance regional jet aircraft under auspice from New Energy Development Organization of Japan (NEDO) since 2003, and then, Mitsubishi Regional Jet (MRJ: Fig. 22) program has been launched by Mitsubishi Aircraft Corp. (MJET) in this spring.[19] In the development of this aircraft,

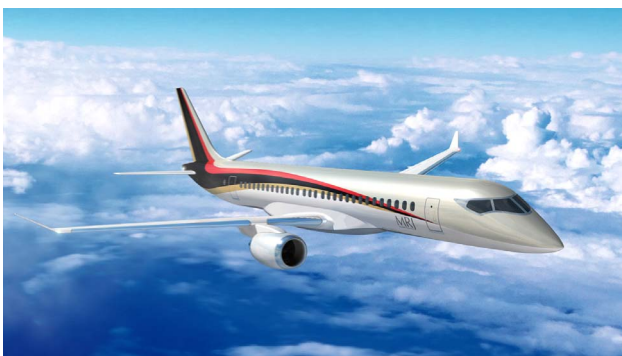


Fig.22. Mitsubishi Regional Jet (MRJ) by MJET

research of airframe noise has been conducted for achieving lower commercial noise as one of the joint research work between MHI and JAXA, and some wind tunnel tests were carried out in LWT1.

At first experiments were conducted on 20%-scale half-span model in LWT1 from 2005 to 2006 as shown in Fig. 23. In this test, the microphone array system was located on the sidewall of the closed test section as same as the system for half-span JSM-HLD model as mentioned above. Figure 24 shows the measurement results of the noise source identification around the main wing of the aircraft model at landing configuration. The results separately identified the noises generated from HLDs and landing gear. Noise characteristics of those sources were evaluated according to frequency, angle of attack, and so on. Especially, it was found that the slat noise was the one of the biggest sound source for the aircraft approach condition. Using these experimental data, the generation mechanism of the slat noise has been calculated by CFD for developing the device that was able to reduce the slat noise.

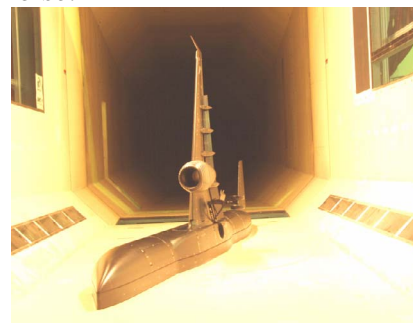


Fig.23. Half-span model of MRJ by MHI

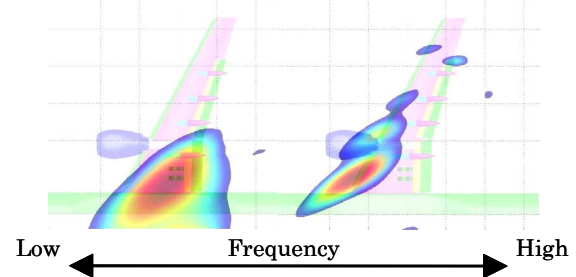


Fig.24. Noise source visualization on MRJ of half-span model

For the other aeroacoustic research for MRJ development, 10%-scale full-span model of MRJ aircraft was also tested in LWT1 in 2007 and 2008 as shown in Fig. 25. In the test, the

microphone array system was located at the ceiling of the test section as same as the system for full-span SST model. The slat noise at the landing configuration was more clearly observed here, especially at high frequency condition shown in Fig. 26. Characteristics of gear noise and flap noise were also evaluated quantitatively. Now, the configuration of HLDs and gears can be modified by using these experimental data, and it will achieve quiet characteristics of the airframe. These noise source data are very useful for the low-noise design of this new MRJ aircraft.

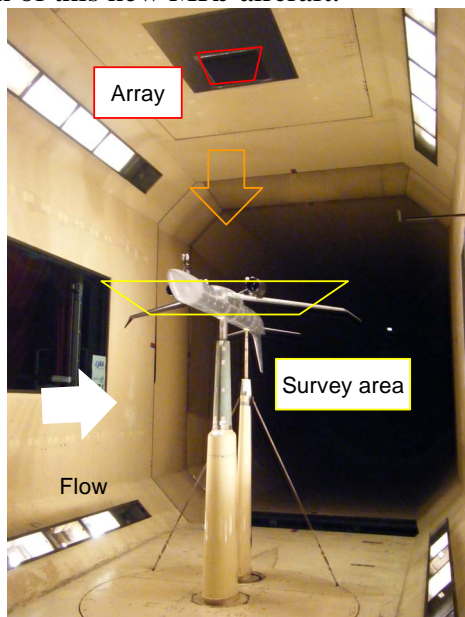


Fig.25. Full-span model of MRJ by MHI with strut support in LWT1

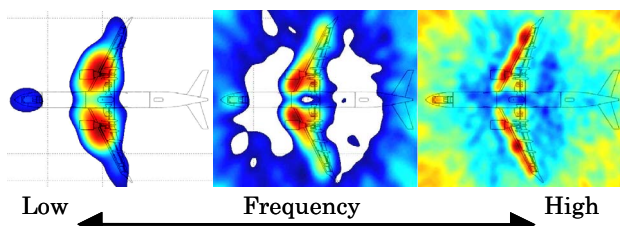


Fig.26. Noise source visualization on MRJ model with strut support

### 5 Concluding remarks

Using phased-array microphone technique, we obtained aerodynamic data in closed test section of conventional aerodynamic wind tunnels. Especially, large-scale testing was carried out, and detailed testing was successfully completed. Aeroacoustic data was able to be discussed with

considering the corresponding aerodynamic data directly in the closed test section. Moreover, some quantitative discussions about contribution by the noise elements will be very useful to search for low noise configuration. These testing techniques are very important feature as the present and future aeroacoustic and aerodynamic design activity.

### Acknowledgement

The authors would like to gratefully thank members of LWT1, LWT2, Civil Transport Team, Supersonic Transport Team in JAXA for their cooperative research works, and also members of aerodynamic testing in MHI for joint research works of large-scale SST model and MRJ model in LWT1.

### References

- [1] Soderman, P. T., "Airframe noise study of a CRJ-700 Aircraft Model in the NASA Ames 7- by 10-foot wind tunnel No.1," AIAA-2002-2406.
- [2] Horne, W.C. et.al., "Measurements of 26%-Scale 777 Airframe Noise in the NASA Ames 40- by 80-ft Wind Tunnel," AIAA-2005-2810.
- [3] Don, H. Johnson, and Dan, E. Dudgeon, "Array Signal Processing," PTR Prentice Hall, 1993.
- [4] Thomas J. Mueller (Ed.), "Aeroacoustic Measurement," Springer, 2001.
- [5] H.Ura, Y.Yokokawa and T.Ito, "Experimental Study of Trailing Edge Noise in Low-speed Wind Tunnel", AIAA-2007-1038.
- [6] M.S.HOWE, "TRAILING EDGE NOISE AT LOW MACH NUMBERS ", Journal of Sound and Vibration, Volume 225, Issue 2, 12 August 1999, Pages 211-238
- [7] A.McAlpine, E.C.Nash and M.V.Lowson, "On the Generation of Discrete Frequency Tones by the Flow around an Aerofoil", Journal of Sound and Vibration, Volume 222, Issue 5, 20 May 1999, Pages 753-779
- [8] Ura, H., Yokokawa, Y., and Ito, T. "Phased Array Measurement of High Lift Devices in Low Speed Wind Tunnel", AIAA-2006-2565
- [9] Yokokawa, Y., Ura, H., Imamura, T., Ito T., and Yamamoto, K. "Detail Observation of Noise and Aerodynamics for High-Lift Configuration Model in JAXA", INTER-NOISE 2007 paper in07-152
- [10] Ura, H., Yokokawa, Y., Imamura, T., Ito, T., and Yamamoto, K."Investigation of Airframe Noise from High Lift Configuration Model", AIAA-2008-19.
- [11] Yokokawa, Y., Imamura, T., Ura, H., Uchida, H., Ito T., and Yamamoto, K. "Studies on airframe noise

- generation at high-lift devices in relation to aerodynamic performance”, AIAA-2008-2960.
- [12]Chow, L.C., et.al., “Landing gears and High Lift Devices Airframe Noise Research,” AIAA-2002-2408
- [13]Alexander R. Quayle et. al. “Landing Gear for a ‘Silent’ Aircraft”, AIAA-2007-231
- [14]Ura,H., Ito,T., Fujita,T., Iwasaki,A., Ando,N. and Sato,J. , ”A Preliminary Study of Landing Gear Noise in Low-Speed Wind Tunnel”, AIAA-2007-3448.
- [15]Yokokawa, Y. et.al., “Experiment and CFD of a High-lift Configuration Civil Transport Aircraft Model”,AIAA-2006-3452
- [16]Ito, T, et al.,” High-Lift Device Testing in JAXA 6.5m x 5.5m Low-speed Wind Tunnel”, AIAA-2006-3463.
- [17]Ito,T., Ura, H., Kajitani, K., Tanaka, H., Igo, K., , ”Aeroacoustic Noise Survey on Supersonic Transport Airframe in Large-scale Aerodynamic Low-speed Wind Tunnel”, AIAA-2008-48.
- [18]Herkes, W.H. and Stoker R.W., “Wind Tunnel Measurements of the Airframe Noise of a High-speed Civil Transport,” AIAA-98-0472.
- [19]Mitsubishi Aircraft Corp., “Mitsubishi Regional Jet “, <http://www.mrj-japan.com/index.html>.

## Copyright Statement

The authors confirm that they, and/or their company or institution, hold copyright on all of the original material included in their paper. They also confirm they have obtained permission, from the copyright holder of any third party material included in their paper, to publish it as part of their paper. The authors grant full permission for the publication and distribution of their paper as part of the ICAS2008 proceedings or as individual off-prints from the proceedings.